

On the Convergence of Semi Unsupervised Calibration through Prior Adaptation Algorithm

Lautaro Estienne^{a,b}, Roberta Hansen^a, Matias Vera^{a,c}, Luciana Ferrer^b,
Pablo Piantanida^d

^a*Facultad de Ingeniería, Universidad de Buenos Aires, Buenos Aires, Argentina*

^b*Instituto de Investigación en Ciencias de la Computación (ICC), CONICET, Buenos Aires, Argentina*

^c*Centro de Simulación Computacional para Aplicaciones Tecnológicas (CSC), CONICET, Buenos Aires, Argentina*

^d*International Laboratory on Learning Systems (ILLS), McGill - ETS - Mila - CNRS - Université Paris Saclay - CentraleSupélec, Montréal, QC, Canada*

Abstract

Calibration is an essential key in machine learning. Semi Unsupervised Calibration through Prior Adaptation (SUCPA) is a calibration algorithm used in (but not limited to) large-scale language models defined by a system of first-order difference equation. The map derived by this system has the peculiarity of being non-hyperbolic with a non-bounded set of non-isolated fixed points. In this work, we prove several convergence properties of this algorithm from the perspective of dynamical systems. For a binary classification problem, it can be shown that the algorithm always converges, more precisely, the map is globally asymptotically stable, and the orbits converge to a single line of fixed points. Finally, we perform numerical experiments on real-world application to support the presented results. Experiment codes are available online¹.

Keywords: Algorithm Convergence, Calibration, Discrete Dynamical Systems

Email addresses: lestienne@fi.uba.ar (Lautaro Estienne), rhansen@fi.uba.ar (Roberta Hansen), mvera@fi.uba.ar (Matias Vera), lferrer@dc.uba.ar (Luciana Ferrer), pablo.piantanida@cnrs.fr (Pablo Piantanida)

¹<https://github.com/LautaroEst/sucpa-convergence>

1. Introduction

First-order difference equations arise in a wide range of disciplines, due to their mathematical simplicity and their adaptability to computerization. Difference equations are generated by maps (functions), which are the main tool for describing discrete time dynamical systems with application to numerical algorithms. Recently, SUCPA algorithm (Semi Unsupervised Calibration through Prior Adaptation) was defined from a first-order non-linear difference equations [10]. This algorithm has applications on calibration of machine learning systems, such as large-scale language models (LLMs).

One of the most important aspect of an algorithm is its convergence properties. An iterative process is said to converge when, as the iterations progress, the output gets closer and closer to a specific solution. Different methods are developed to demonstrate the convergence of algorithms depending on the discipline in which they are applied, and it is an always current topic ([1, 17, 4], just to name a few). The main objective of this work is to study the convergence of the SUCPA algorithm using dynamical systems analysis techniques. The map defined by this algorithm has the particularity of being non-hyperbolic and its fixed points (the solutions to which the algorithm converges) form an unbounded set of non-isolated points, so the stability problem cannot be addressed by the usual local linearization techniques, and it requires a certain craftsmanship to be solved.

As detailed in [10], the SUCPA algorithm was first developed to correct the scores outputted by a supervised machine learning classifier. In the context of Statistical Learning, the goal of a supervised learning algorithm is to estimate a function that maps an input (e.g., an image or a text) to an output (e.g., a label from a pre-defined set of categories). This estimation is done with a set of training data, which contains examples of input-output pairs, and gives the function to be used with new data as a result. This mapping is usually done in two steps: first, the probability distribution of an output given the input is estimated from the training set, and then, the output is predicted as the one with the highest probability. It is a well known result that once the conditional probability distribution over the predefined categories given the input is known it is trivial to map the input to the label that minimizes the Bayes Risk [8], which is a standard criterion for optimality.

However, because of how they are obtained, the estimated probabilities of most modern classifiers do not always represent the probability distribution

of the data in which the classifier will be used [11]. For instance, many of these classifiers are first pre-trained on a massive training set and then they are adapted to a downstream task [7, 15]. If this adaptation step is not done correctly, it may lead to a classifier that is not well calibrated, i.e., the estimated probabilities of the classifier may not represent the probability distribution of the data in which the classifier will be used, which may lead to sub-optimal performance, according to the Bayes criterion mentioned above.

Despite that most modern classifier are not usually calibrated, there are multiple methods to calibrate them [5]. SUCPA algorithm is a semi-unsupervised example of these methods, where even though no labelled data is available, the class priors (proportions of samples in each class) can be known or estimated from knowledge of the task. This algorithm has the feature of being computationally really simple and achieving good performance for LLMs [10].

In the present work the convergence of SUCPA algorithm is studied. We prove the convergence for the two-classes case, and show different properties and conjectures of the general case. The paper is organized as follows. In Section 2 we explain the foundations of the algorithm, its mathematical definition and the basic elements to interpret it. Section 3 summarizes some essential properties of the algorithm. In Section 4 we prove the convergence for two classes. Numerical examples are shown in Section 5. Finally, in Section 6, some concluding remarks are discussed.

2. Problem Description

In this section we formally introduce the SUCPA map to be studied. In order to understand the origin of this map, we briefly describe the SUCPA algorithm in Section 2.1 and define some useful elements in Section 2.2.

2.1. Understanding SUCPA algorithm

One of the most popular calibration methods is Logistic Regression [2], in which it is assumed that the calibrated probability $\tilde{P}(k|\mathbf{x})$ of a class k , $k=1, \dots, K$ given an input \mathbf{x} is related to the estimated probability $P(k|\mathbf{x})$ by an affine transformation in the log-domain:

$$\log \tilde{P}(k|\mathbf{x}) = \alpha_k \log P(k|\mathbf{x}) + \beta_k + \gamma(\boldsymbol{\alpha}, \boldsymbol{\beta}), \quad (1)$$

where $\boldsymbol{\alpha} = [\alpha_1, \dots, \alpha_K]$, $\boldsymbol{\beta} = [\beta_1, \dots, \beta_K]$ and $\gamma(\boldsymbol{\alpha}, \boldsymbol{\beta})$ is determined so that $\sum_{k=1}^K \tilde{P}(k|\mathbf{x}) = 1$. Here, $\boldsymbol{\alpha}$ and $\boldsymbol{\beta}$ are parameters of the affine transformation

and they are trained using a Proper Scoring Rule (usually the Negative Log-Likelihood or *cross-entropy*) [5].

Different assumptions in equation 1 are usually made according to the specific problem that needs to be solved. For instance, temperature scaling [11], one of the most widely used calibration methods, corresponds to taking $\beta_k = 0$ for all k and $\alpha_k = \frac{1}{T}$ a single scalar. In contrast to this, SUCPA algorithm is derived for the case in which $\alpha_k = 1$ for all $k \in \{1, \dots, K\}$ because it is assumed that the probabilities that are expected to find in practice have different priors than the ones used to train the model [3, 14]. Now, if we restrict the calibration transformation to $\alpha_k = 1$ for all k , SUCPA algorithm minimize the following cross-entropy for a given a dataset $\mathcal{D} = \{(\mathbf{x}_1, y_1), \dots, (\mathbf{x}_N, y_N)\}$ where $y_i \in \{k=1, \dots, K\}$:

$$\mathcal{L}(\boldsymbol{\beta}) = \frac{1}{N} \sum_{i=1}^N -\log \tilde{P}(y_i | \mathbf{x}_i) \quad (2)$$

$$= -\frac{1}{N} \sum_{i=1}^N [\log P(y_i | \mathbf{x}_i) + \beta_{y_i} + \gamma_i(\mathbf{1}, \boldsymbol{\beta})] \quad (3)$$

If we set the derivative of the cross-entropy to zero, we can derive the following expression for β_k :

$$\beta_k = \log \left(\frac{N_k}{N} \right) - \left(\frac{1}{N} \sum_{i=1}^N \frac{P(k | \mathbf{x}_i)}{\sum_{j=1}^K P(j | \mathbf{x}_i) e^{\beta_j}} \right) \quad (4)$$

where N_k is the number of samples with $y_i = k$. Mathematical details can be read in [10]. If the proportion $\frac{N_k}{N}$ is known as a consequence of some previous estimation or external knowledge from the nature of the task, then equation 4 can be used to estimate the value of β_k for every $k \in \{1, \dots, K\}$ using just the samples $\{\mathbf{x}_1, \dots, \mathbf{x}_N\}$ (i.e., with no labels). This is done using the SUCPA algorithm (see algorithm 1).

2.2. Problem definition

The following definition introduces the SUCPA map, to be studied in this work.

Definition 1. Let $\boldsymbol{\beta}^{[t]} = [\beta_1^{[t]}, \dots, \beta_K^{[t]}] \in \mathbb{R}^K$ and $\boldsymbol{\beta}^{[0]} \in \mathbb{R}^K$ be an initial condition. Let also, $[N_1, \dots, N_K] \in \mathbb{N}^K$, with $\sum_{k=1}^K N_k = N$ and $\mathbf{P} \in \mathbb{R}^{N \times K}$

Algorithm 1 SUCPA

Require: s (number of steps) , $\beta_1^{[0]}, \dots, \beta_K^{[0]}$ (starting values)

Ensure: $\beta_1^*, \dots, \beta_K^*$

for k **in** $1, \dots, K$ **do**

$\beta_k \leftarrow \beta_k^{[0]}$

end for

$t \leftarrow 0$

while $t \leq s$ **do**

for k **in** $1, \dots, K$ **do**

$$\beta_k \leftarrow -\log \left(\frac{1}{N_k} \sum_{i=1}^N \frac{P_{i,k}}{\sum_{j=1}^K P_{i,j} e^{\beta_j}} \right)$$

end for

$t \leftarrow t + 1$

end while

for k **in** $1, \dots, K$ **do**

$\beta_k^* \leftarrow \beta_k$

end for

a matrix which coefficients meet $P_{i,k} > 0$ and $\sum_{k=1}^K P_{i,k} = 1$. We define the SUCPA algorithm as:

$$\beta_k^{[t+1]} = -\log \left(\frac{1}{N_k} \sum_{i=1}^N \frac{P_{i,k}}{\sum_{j=1}^K P_{i,j} e^{\beta_j^{[t]}}} \right). \quad (5)$$

Let $\mathbf{f} = [f_1, \dots, f_K] : \mathbb{R}^K \rightarrow \mathbb{R}^K$, the map defined by (5), $\beta^{[t+1]} = \mathbf{f}(\beta^{[t]})$, with:

$$f_k(\beta) = -\log \left(\frac{1}{N_k} \sum_{i=1}^N \frac{P_{i,k}}{\sum_{j=1}^K P_{i,j} e^{\beta_j}} \right). \quad (6)$$

Let $\mathbf{f}^{(t+1)}(\beta) = \mathbf{f}(\mathbf{f}^{(t)}(\beta))$ with $t \in \mathbb{N}$, $\mathbf{f}^{(1)}(\beta) = \mathbf{f}(\beta)$ and $\mathbf{f}^{(0)}(\beta) = \beta$.

In order to study the aforementioned map, we need to introduce some basic definitions.

Definition 2. Let \mathbf{f} a map; we define,

1. $\beta^* \in \mathbb{R}^K$ is a fixed point if it verifies $\mathbf{f}(\beta^*) = \beta^*$.

2. We call ω -limit set of β to,

$$\omega(\beta) = \bigcap_{n=0}^{\infty} \overline{\{\mathbf{f}^{(t)}(\beta), t \geq n\}} \quad (7)$$

where the over-bar accounts for the closure of a set.

The fixed points can be interpreted as points that do not vary when undergoing iterations of the algorithm, and the ω -limit of β is the set of points where the algorithm, started in β , converges with the successive iterations.

Remark 1. *The ω -limit set is a limit set because it is the intersection of nonincreasing sets. They are always closed sets (intersection of closed sets is closed), and they can be of different type: a single point, a periodic orbit, an infinite set, an unbounded set, an empty set, and can have also complicated structures [20].*

In this work we study several properties of the SUCPA algorithm. In particular, we are interested in focusing on the convergence of the algorithm for any initial condition (i.c.), $\beta^{[0]} \in \mathbb{R}^K$.

Conjecture 1. *For each i.c. $\beta^{[0]}$, there exist a unique fixed point, $\beta^* \in \mathbb{R}^K$ ($\beta^*(\beta^{[0]})$), such that $\omega(\beta^{[0]}) = \{\beta^*\}$ (it is a single point set).*

The general case of $K \in \mathbb{N}$ of this conjecture is not yet proven, although many interesting properties have been revealed. However, the particular case of $K = 2$ is completely proven and reported in this work.

3. Main properties of SUCPA algorithm

Within the literature of discrete dynamical systems, most problems deal with the stability of *isolated* fixed points. A fixed point is called isolated, if there exists a neighborhood of the fixed point that does not contain any other fixed points, otherwise it is called *non-isolated*. The standard tools to study both, local and global stability focus on the linearization of the system at those points, and/or obtaining the so-called Lyapunov functions [6, 20]. Furthermore, the number of fixed points is usually finite and therefore a bounded set results. In our case, on the contrary, the system defined in (5) presents, by the way, a fairly simple behavior in the sense of its dynamics (for example, there is no presence of chaos despite its non-linearity). However, as

we will see, the fixed points of the system make up a non-bounded set of non-isolated points. Indeed, the set of fixed points is a straight line. These two unusual features together with the no so simple algebraic equations, make the study of the system stability to be approached in other ways, by defining *ad hoc* auxiliary functions and solving it in a more artisanal way, at least in the case $K=2$.

3.1. Fixed points analysis

The map presented in (6) has a particular behavior against constant vector sums. It is not hard to see the following result.

Lemma 1. *Let $\boldsymbol{\lambda} = [\lambda, \dots, \lambda] \in \mathbb{R}^K$ a constant vector (all entries are equal), then, the map \mathbf{f} defined in (6) satisfies:*

$$\mathbf{f}(\boldsymbol{\beta} + \boldsymbol{\lambda}) = \mathbf{f}(\boldsymbol{\beta}) + \boldsymbol{\lambda} \quad (8)$$

Proof. It is straightforward evaluating (6) in $\boldsymbol{\beta} + \boldsymbol{\lambda}$. \square

Naturally, this feature remains valid under successive iterations of \mathbf{f} . This implies the following geometry for the set of fixed points.

Corollary 1. *Let $\boldsymbol{\lambda} = [\lambda, \dots, \lambda] \in \mathbb{R}^K$. If $\boldsymbol{\beta}^*$ is a fixed point of the map \mathbf{f} , then the points in the straight line, $\mathcal{S}(\boldsymbol{\beta}^*)$, of the form:*

$$\mathcal{S}(\boldsymbol{\beta}^*) = \{\boldsymbol{\beta} = \boldsymbol{\lambda} + \boldsymbol{\beta}^*, \lambda \in \mathbb{R}\} \quad (9)$$

are also fixed points of the system (6).

Proof. We start to prove $\mathbf{f}^{(t)}(\boldsymbol{\beta} + \boldsymbol{\lambda}) = \mathbf{f}^{(t)}(\boldsymbol{\beta}) + \boldsymbol{\lambda}$ for all $t \geq 1$ via induction. For $t=1$, the statement is the Lemma 1. Assuming $\mathbf{f}^{(t)}(\boldsymbol{\beta} + \boldsymbol{\lambda}) = \mathbf{f}^{(t)}(\boldsymbol{\beta}) + \boldsymbol{\lambda}$ is valid, then for $t+1$:

$$\mathbf{f}^{(t+1)}(\boldsymbol{\beta} + \boldsymbol{\lambda}) = \mathbf{f}(\mathbf{f}^{(t)}(\boldsymbol{\beta} + \boldsymbol{\lambda})) = \mathbf{f}(\mathbf{f}^{(t)}(\boldsymbol{\beta}) + \boldsymbol{\lambda}) = \mathbf{f}^{(t+1)}(\boldsymbol{\beta}) + \boldsymbol{\lambda} \quad (10)$$

\square

This result shows that if the algorithm converges to $\boldsymbol{\beta}^*$ for some initial condition $\boldsymbol{\beta}^{[0]}$, then it converges to $\boldsymbol{\beta}^* + \boldsymbol{\lambda}$ when the initial condition is $\boldsymbol{\beta}^{[0]} + \boldsymbol{\lambda}$ (an example can be seen in Fig. 3). If $\boldsymbol{\beta}^*$ is a fixed point, the points of the straight line of $\mathbf{1} = [1, \dots, 1]$ direction and through $\boldsymbol{\beta}^*$ are also fixed points.

There is numerical evidence to formulate the following conjecture, although only the case $K=2$ is demonstrated.

Conjecture 2. *There exists a unique straight line of fixed points of \mathbf{f} , and it is of the form (9).*

3.2. Jacobian Matrix analysis

The Jacobian matrix of a system is an essential feature to study, for example, the local dynamics around the fixed points of a map [6, 20].

The Jacobian matrix, $\mathbf{J}(\boldsymbol{\beta})$, of the map \mathbf{f} defined in (6) evaluated at $\boldsymbol{\beta}$, is the matrix whose elements, $J_{k,\ell}(\boldsymbol{\beta}) = \frac{\partial f_k}{\partial \beta_\ell}(\boldsymbol{\beta})$, with $k, \ell = 1, \dots, K$, can be computed as:

$$J_{k,\ell}(\boldsymbol{\beta}) = \frac{\sum_{i=1}^N \frac{P_{i,k} P_{i,\ell} e^{\beta_\ell}}{\left(\sum_{j=1}^K P_{i,j} e^{\beta_j} \right)^2}}{\sum_{i=1}^N \frac{P_{i,k}}{\sum_{j=1}^K P_{i,j} e^{\beta_j}}} \quad (11)$$

In particular, $\mathbf{J}(\boldsymbol{\beta})$ turns to be a *regular transition probability matrix* for all $\boldsymbol{\beta} \in \mathbb{R}^K$, and so, it has the following properties:

Lemma 2. *The Jacobian matrix defined by the elements of (12) achieves the following properties:*

- (i) $J_{k,\ell}(\boldsymbol{\beta}) > 0, \forall k, \ell$
- (ii) *Each row of the matrix adds up to 1, i.e.:*

$$\sum_{\ell=1}^K J_{k,\ell}(\boldsymbol{\beta}) = 1, \forall 1 \leq k \leq K \quad (12)$$

This condition necessarily means that $\mathbf{J}(\boldsymbol{\beta})$ has an eigenvalue $\mu = 1$ with an associated eigenvector $\mathbf{1} = [1, \dots, 1]$.

- (iii) $\mu = 1$ has multiplicity one, and all others eigenvalues verify $|\mu| < 1$.

Proof. Items (i) and (ii) are straightforward to prove. Item (iii) is consequence of Perron's Theo. [13, Chapter 8]. \square

3.3. Other definitions and results

The results presented above will now be complemented with additional definitions and complementary results.

3.3.1. Some extra definitions

To deepen into some additional details, we add some necessary concepts.

Definition 3. *The forward orbit of $\beta \in \mathbb{R}^K$ is the set*

$$O^+(\beta) = \{\mathbf{f}^{(t)}(\beta), t \in \mathbb{N} \cup \{0\}\} \quad (13)$$

The forward orbit of β is the set of all points that the algorithm will pass through when starting at β .

Definition 4. $\mathcal{X} \subset \mathbb{R}^K$ is an invariant set if $\mathbf{f}(\mathcal{X}) \subset \mathcal{X}$. If $\mathbf{f}(\mathcal{X}) = \mathcal{X}$, \mathcal{X} is called strongly invariant (or s-invariant for short).

This means that all forward orbits of points in \mathcal{X} lie in \mathcal{X} . In particular, any set of fixed points is s-invariant. Also, for all β , the set $\omega(\beta)$ is a s-invariant set.

Definition 5. A fixed point β^* of a map \mathbf{f} , is called unstable, if at least one eigenvalue of $\mathbf{J}(\beta^*)$ has modulus greater than one. Otherwise, it is called stable. If all eigenvalues have modulus less than one, it is called asymptotically stable.

3.3.2. Additional Results

The system presented in (5) has different properties. The first result to mention is the fixed point analysis. According to Definition 2.1, and (6), β^* is a fixed point for \mathbf{f} , if and only if:

$$e^{-\beta_k^*} = \frac{1}{N_k} \sum_{i=1}^N \frac{P_{i,k}}{\sum_{j=1}^K P_{i,j} e^{\beta_j^*}} \quad \forall k = 1, \dots, K. \quad (14)$$

The following Lemma is related to the increments of an orbit.

Lemma 3. *Let $\Delta_k(t) = \beta_k^{[t+1]} - \beta_k^{[t]}$. Then, the following condition holds:*

$$\sum_{k=1}^K N_k e^{-\Delta_k(t)} = N \quad (15)$$

Proof. It is not hard to see that each $\Delta_k(t)$ can be written as:

$$\Delta_k(t) = -\log \left(\frac{1}{N_k} \sum_{i=1}^N \frac{P_{i,k} e^{\beta_k^{[t]}}}{\sum_{j=1}^K P_{i,j} e^{\beta_j^{[t]}}} \right) \quad (16)$$

So, it is necessary to meet:

$$N_k e^{-\Delta_k(t)} = \sum_{i=1}^N \frac{P_{i,k} e^{\beta_k^{[t]}}}{\sum_{j=1}^K P_{i,j} e^{\beta_j^{[t]}}} \quad (17)$$

Adding term to term over k , the proof is over. \square

Lemma 3 shows that the results of the algorithm values in every step are, in some sense, in balance, since, if for some k , β_k tends to increase with the iterations, then there must be, at least, another k' , for which $\beta_{k'}$ tend to decrease (and vice versa).

4. The case of two classes

For $K = 2$, $\beta = [\beta_1, \beta_2]$, the SUCPA algorithm (5), and the map $\mathbf{f} = [f_1, f_2]:\mathbb{R}^2 \rightarrow \mathbb{R}^2$, become into:

$$\begin{cases} f_1(\beta^{[t]}) = \beta_1^{[t+1]} = -\log \left(\frac{1}{N_1} \sum_{i=1}^N \frac{P_{i,1}}{P_{i,1} e^{\beta_1^{[t]}} + P_{i,2} e^{\beta_2^{[t]}}} \right) \\ f_2(\beta^{[t]}) = \beta_2^{[t+1]} = -\log \left(\frac{1}{N_2} \sum_{i=1}^N \frac{P_{i,2}}{P_{i,1} e^{\beta_1^{[t]}} + P_{i,2} e^{\beta_2^{[t]}}} \right) \end{cases} \quad (18)$$

where $N_1 + N_2 = N$, $P_{i,1} > 0$ and $P_{i,1} + P_{i,2} = 1$, for all $i = 1, \dots, N$. Furthermore, the technical Lemma 3 can be reduced to

$$N_1 e^{-\Delta_1(t)} + N_2 e^{-\Delta_2(t)} = N \quad (19)$$

where $\Delta_1(t) = \beta_1^{[t+1]} - \beta_1^{[t]}$ and $\Delta_2(t) = \beta_2^{[t+1]} - \beta_2^{[t]}$.

Definition 6. For $x \in \mathbb{R}$, let \mathcal{S}_x be the straight line with slope 1 and cross the y -axis at x value:

$$\mathcal{S}_x = \{\beta = [\lambda, \lambda + x], \lambda \in \mathbb{R}\} \quad (20)$$

Note that the straight lines of fixed point to be found are of this type, and so, will be determined only by their intercepts.

4.1. Main results

When $K = 2$, there are other properties of the map. The results will be splitted up into those related to convergence and those related to the Jacobian matrix.

4.1.1. About the convergence

As said before, Conjectures 1 and 2 can be proven when the number of classes $K=2$. The main result can be stated as follow: *There exists a unique straight line built up by fixed points, to which the algorithm converges, for all initialization.* In terms of dynamical systems, this is equivalent to state the following theorems.

Theorem 1. *Let \mathbf{f} be the map defined in (6) for $K=2$. Then, there exists a unique $b \in \mathbb{R}$, such that the fixed point set of \mathbf{f} is \mathcal{S}_b .*

Note that the fixed point are not-isolated points, and they make up a set, \mathcal{S}_b , which is also unbounded.

Theorem 2. *Let \mathbf{f} be the map defined in (6) for $K=2$. For all initial conditions $\boldsymbol{\beta}^{[0]}$, there exist a fixed point, $\boldsymbol{\beta}^* \in \mathbb{R}^2$ ($\boldsymbol{\beta}^*(\boldsymbol{\beta}^{[0]})$), such that $\omega(\boldsymbol{\beta}^{[0]}) = \{\boldsymbol{\beta}^*\}$.*

Both proofs can be seen in Section 4.1.3 and 4.2.4, respectively. In addition, once it is known that the algorithm must be convergent, it is necessary that $\Delta_1(t)$ and $\Delta_2(t)$ go to zero when $t \rightarrow \infty$. From (19), and applying the L'Hopital's rule, it can be obtained the direction of convergence:

$$\lim_{t \rightarrow +\infty} \frac{\Delta_2(t)}{\Delta_1(t)} = \lim_{\Delta_1 \rightarrow 0} \frac{-\log\left(\frac{N - N_1 e^{-\Delta_1}}{N_2}\right)}{\Delta_1} \quad (21)$$

$$= \lim_{\Delta_1 \rightarrow 0} \frac{-N_2}{(N - N_1 e^{-\Delta_1})} \frac{N_1}{N_2} e^{-\Delta_1} \quad (22)$$

$$= -\frac{N_1}{N_2} \quad (23)$$

This result means that $O^+(\boldsymbol{\beta}^{[0]})$ becomes tangent to a straight line of slope $-N_1/N_2$.

4.1.2. About the Jacobian matrix

It is known that the eigenvalues and eigenvectors of the Jacobian matrix of a map, evaluated at a fixed point, account for the local dynamics of the system around that point, and hence the importance of obtaining them.

Roughly speaking, a fixed point $\boldsymbol{\beta}^*$ of a map \mathbf{f} is call *hyperbolic*, if the Jacobian matrix, $\mathbf{J}_\mathbf{f}(\boldsymbol{\beta}^*)$, has no eigenvalues, μ , of modulus one. Otherwise,

it is called *nonhyperbolic*. The invariant spaces, E^s , E^u and E^c , of $\mathbf{J}_f(\beta^*)$, associated to $|\mu| > 1$, $|\mu| < 1$ and $|\mu| = 1$, respectively, correspond to the *local* stable, the *local* unstable and the *local* “central” directions, respectively [6, 20].

By Lemma 2, the two eigenvalues of $\mathbf{J}_f(\beta^*)$ are, 1 with associated eigenvector $\mathbf{1}$, and the other, μ , must verify $|\mu| < 1$, so, the fixed points are all of nonhyperbolic type. The eigenvalue 1 is in accordance with the obtaining of non-isolated fixed points [19], and the eigenvector $\mathbf{1}$ is in accordance with the direction of the line of fixed points. Therefore, $E^u = \emptyset$, $E^c = \text{span}\{\mathbf{1}\}$ and $E^s = \text{span}\{\mathbf{v}\}$, with \mathbf{v} to be determined, is the eigenvector associated to μ . The following lemma shows some features for the eigen-pair of the Jacobian matrix for the fixed points.

Lemma 4. *Let $\beta^* \in \mathbb{R}^2$ a fixed point of f . The eigen-pairs of $\mathbf{J}_f(\beta^*)$ are $(1, \mathbf{1})$ and (μ, \mathbf{v}) where:*

- (i) *The value of μ and \mathbf{v} are the same for all fixed point β^**
- (ii) *$0 \leq \mu < 1$*
- (iii) *$\mathbf{v} = [N_2, -N_1]$*

The proof can be seen in Section 4.2.3. Fig. 1 illustrate the phase portrait of the local dynamics near \mathcal{S}_b . Note that the eigenvalues and eigenvectors of the Jacobian matrix of a map, evaluated at a fixed point, account for the local dynamics of the system around that point. So, it is not hard to see that every point $\beta^* \in \mathcal{S}_b$ is stable, which means that there exists a neighborhood of β^* , say $B(\beta^*, \varepsilon)$, for some $\varepsilon > 0$, such that every orbit that enters it, stays there. Besides, as the ε value is the same for all the fixed points (because the Jacobian matrix is), it turns out that the set:

$$\mathcal{S}_b(\varepsilon) = \bigcup_{\beta^* \in \mathcal{S}_b} B(\beta^*, \varepsilon) \quad (24)$$

is an invariant set for the map f . The set $\mathcal{S}_b(\varepsilon)$ is nothing but the strip of 2ε -width around \mathcal{S}_b , and the dynamics within it will be characterize by the sign of μ (see Fig. 1).

In the following section we introduce some auxiliary functions useful to understand the dynamics of the map.

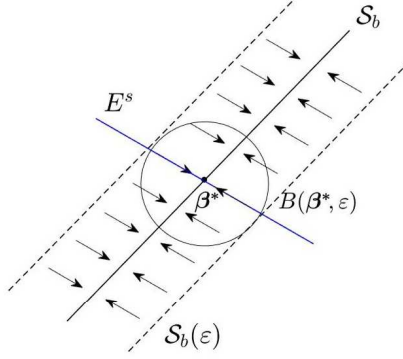


Figure 1: Schematic representation of local stability at a fixed point $\beta^* \in S_b$ within a ball of radius ϵ centered at β^* . The stability direction E^s (blue line). The direction of E^c matches that of the S_b . The dynamics is a replica for all fixed point on S_b and within the 2ϵ -width strip $S_b(\epsilon)$.

4.1.3. Auxiliary functions and its properties

In order to prove the main results, we define the following two functions which will be very useful in the technical details of the demonstration. Let $\alpha_1, \alpha_2: \mathbb{R} \rightarrow \mathbb{R}$ be two function defined for x as:

$$\alpha_1(x) = \frac{1}{N_1} \sum_{i=1}^N \frac{P_{i,1}}{P_{i,1} + P_{i,2} e^x}, \quad \alpha_2(x) = \frac{1}{N_2} \sum_{i=1}^N \frac{P_{i,2}}{P_{i,1} + P_{i,2} e^x} \quad (25)$$

The functions $\alpha_k(x)$, $k = 1, 2$, are positive and continuous derivable. They also satisfy the following relation, for $x \in \mathbb{R}$:

$$N_1 \alpha_1(x) + N_2 e^x \alpha_2(x) = N \quad (26)$$

Lemma 5. $\alpha_k(x)$ are monotone decreasing on x , $k=1, 2$.

Proof. Indeed, for all $x \in \mathbb{R}$:

$$\alpha'_1(x) = \frac{1}{N_1} \sum_{i=1}^N \frac{-P_{i,1} P_{i,2} e^x}{(P_{i,1} + P_{i,2} e^x)^2} < 0 \quad \alpha'_2(x) = \frac{1}{N_2} \sum_{i=1}^N \frac{-P_{i,2}^2 e^x}{(P_{i,1} + P_{i,2} e^x)^2} < 0 \quad (27)$$

□

4.2. Proofs of the main results

Proofs of the previously mentioned results are developed below. Among them, Theo. 1, Theo. 2 and Lemma 4 stand out.

4.2.1. Proof of Theo. 1

Corollary 1 shows that, if there exists a fixed point, the points on the line of unit slope that passes through said fixed point are also fixed points. These straight lines are defined from their intercept b , defining the line \mathcal{S}_b . Let $\beta^* = [\beta_1^*, \beta_2^*]$ be a fixed point. By the unitary slope, the intercept is the value, $b = \beta_2 - \beta_1$, which must satisfy (14).

Using the auxiliary functions defined in the Section 4.1.3, Theo. 1 is equivalent to state that there exists a unique value $b \in \mathbb{R}$, such that $\alpha_1(b) = 1$ and $\alpha_2(b) = e^{-b}$.

Indeed, taking limits in (25), for $x \rightarrow -\infty$ and for $x \rightarrow +\infty$ respectively, it is obtained:

$$\lim_{x \rightarrow -\infty} \alpha_1(x) = \lim_{x \rightarrow -\infty} \frac{1}{N_1} \sum_{i=1}^N \frac{P_{i,1}}{P_{i,1} + P_{i,2} e^x} = \frac{N}{N_1} > 1 \quad (28)$$

$$\lim_{x \rightarrow +\infty} \alpha_1(x) = \lim_{x \rightarrow +\infty} \frac{1}{N_2} \sum_{i=1}^N \frac{P_{i,1}}{P_{i,1} + P_{i,2} e^x} = 0 < 1 \quad (29)$$

The conclusion follows from the mean value theorem and the uniqueness from the α_1 strict monotony. The proof of $\alpha_2(b) = e^{-b}$ comes straight out from (26).

4.2.2. About the intercepts

For every point $\beta = [\beta_1, \beta_2] \in \mathbb{R}^2$ there is a single straight line, \mathcal{S}_x , of slope 1 and intercept, $x = \beta_2 - \beta_1$, that passes through it. This section is devoted to show that every \mathcal{S}_x monotonously approaches to \mathcal{S}_b , where b is the intercept of the fixed points line. In this context, (14) implies:

$$\beta_2^{[t+1]} - \beta_1^{[t+1]} = \log \left(\frac{\alpha_1(\beta_2^{[t]} - \beta_1^{[t]})}{\alpha_2(\beta_2^{[t]} - \beta_1^{[t]})} \right) \quad (30)$$

For each $x \in \mathbb{R}$, the function $\phi(x) = \log \left(\frac{\alpha_1(x)}{\alpha_2(x)} \right)$, defines the update of the intercepts according to the iterations. In particular, for the fixed points, this relationship implies:

$$b = \phi(b) = \log \left(\frac{\alpha_1(b)}{\alpha_2(b)} \right) \quad (31)$$

The following lemma shows the monotonously approaches of the intercept to b .

Lemma 6.

(i) For $x > b$: $b \leq \phi(x) < x$

(ii) For $x < b$: $x < \phi(x) \leq b$

Proof. The right inequality in Lemma 6 (i) is fairly straightforward to prove. By Lemma 5 and (29), we have $\alpha_1(x) < 1 = \alpha_1(b)$, and then, (26) implies $e^x \alpha_2(x) > 1$. Thus, $\alpha_1(x) < e^x \alpha_2(x)$, that results equivalent to the statement ($\alpha_2(x) > 0$).

To obtain the left inequality, we must “split hair”. It is equivalent to prove:

$$\frac{\alpha_2(x)}{\alpha_1(x)} \leq e^{-b} \quad (32)$$

Let g be a function on x defined as:

$$g(x) = e^{\phi(x)} = \frac{\alpha_2(x)}{\alpha_1(x)} \quad (33)$$

Note that $g(b) = e^{-b}$, via (31). Thus, to obtain (32), all that remains is to prove that g is a monotone non-increasing function, i.e., $g'(x) \leq 0$, for all $x > b$. This is equivalent to show that:

$$N_1 N_2 (\alpha'_2(x) \alpha_1(x) - \alpha'_1(x) \alpha_2(x)) \leq 0 \quad (34)$$

By using the expressions of α_k and α'_k in 25 and 27:

$$\begin{aligned} & N_1 N_2 \alpha'_2(x) \alpha_1(x) - N_1 N_2 \alpha'_1(x) \alpha_2(x) \\ &= \left[\sum_{i=1}^N \frac{-P_{i,2}^2 e^x}{(P_{i,1} + P_{i,2} e^x)^2} \right] \left[\sum_{j=1}^N \frac{P_{j,1}}{P_{j,1} + P_{j,2} e^x} \right] \\ &\quad - \left[\sum_{i=1}^N \frac{-P_{i,1} P_{i,2} e^x}{(P_{i,1} + P_{i,2} e^x)^2} \right] \left[\sum_{j=1}^N \frac{P_{j,2}}{P_{j,1} + P_{j,2} e^x} \right] \end{aligned} \quad (35)$$

$$= \sum_{j=1}^N \sum_{i=1}^N \frac{-P_{i,2}^2 e^x P_{j,1} + P_{i,1} P_{i,2} e^x P_{j,2}}{(P_{i,1} + P_{i,2} e^x)^2 (P_{j,1} + P_{j,2} e^x)} \quad (36)$$

$$= e^x \sum_{j=1}^N \sum_{i=1}^N \frac{P_{i,2} (P_{i,1} P_{j,2} - P_{i,2} P_{j,1})}{(P_{i,1} + P_{i,2} e^x)^2 (P_{j,1} + P_{j,2} e^x)} \quad (37)$$

$$= e^x \sum_{j=1}^N \sum_{i=1}^N \frac{P_{i,2} (P_{i,1} P_{j,2} - P_{i,2} P_{j,1}) (P_{j,1} + P_{j,2} e^x)}{(P_{i,1} + P_{i,2} e^x)^2 (P_{j,1} + P_{j,2} e^x)^2} \quad (38)$$

The terms with $i=j$ in the last expression, equal zero. For $i \neq j$, since what matters is the sign of (35), we proceed by adding two symmetric terms on i and j , and taking into account only the numerators:

$$P_{i,2} (P_{i,1}P_{j,2} - P_{i,2}P_{j,1}) (P_{j,1} + P_{j,2}e^x) + P_{j,2} (P_{j,1}P_{i,2} - P_{j,2}P_{i,1}) (P_{i,1} + P_{i,2}e^x) \\ = (P_{i,1}P_{j,2} - P_{i,2}P_{j,1}) [P_{i,2} (P_{j,1} + P_{j,2}e^x) - P_{j,2} (P_{i,1} + P_{i,2}e^x)] \quad (39)$$

$$= (P_{i,1}P_{j,2} - P_{i,2}P_{j,1}) [P_{i,2}P_{j,1} + P_{i,2}P_{j,2}e^x - P_{j,2}P_{i,1} - P_{j,2}P_{i,2}e^x] \quad (40)$$

$$= -(P_{i,1}P_{j,2} - P_{i,2}P_{j,1})^2 \leq 0 \quad (41)$$

Then, (34) holds, $g'(x) \leq 0$ and $g(x) \leq e^{-b}$. In an analogous way, it can be proven the same inequalities corresponding to Lemma 6 (ii), for $x < b$. \square

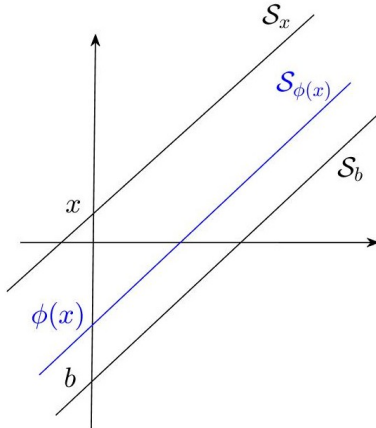


Figure 2: Any unitary slope straight line \mathcal{S}_x above the line of fixed points, \mathcal{S}_b , is mapped onto another one, $\mathbf{f}(\mathcal{S}_x) = \mathcal{S}_{\phi(x)}$ (in blue), placed between them, but strictly above \mathcal{S}_x .

The geometrical interpretation of this lemma is the following. Let's call \mathcal{S}_b^\uparrow and \mathcal{S}_b^\downarrow , the semi-planes located above and below \mathcal{S}_b , respectively, then they are invariant sets for \mathbf{f} .

Corollary 2. *If $\beta \in \mathcal{S}_b^\uparrow$, then $O^+(\beta) \in \mathcal{S}_b^\uparrow$, and if $\beta \in \mathcal{S}_b^\downarrow$, then $O^+(\beta) \in \mathcal{S}_b^\downarrow$.*

Moreover, if $x > b$ (the straight line \mathcal{S}_x is placed above the fixed straight line \mathcal{S}_b), then, Lemma 6 states that $\mathcal{S}_{\phi(x)}$ will be placed between \mathcal{S}_x and \mathcal{S}_b , but *strictly* under the first one. See Fig. 2.

4.2.3. Proof of Lemma 4

Theo. 1 implies that there exists a unique value $b \in \mathbb{R}$, such that $\alpha_1(b) = 1$ and $\alpha_2(b) = e^{-b}$. In this context, the Jacobian matrix of the map \mathbf{f} , defined in (11), and evaluated at fixed points, $\beta^* = [\lambda, \lambda+b]$, becomes:

$$\mathbf{J}_b = \mathbf{J}_f([\lambda, \lambda+b]) = \begin{bmatrix} \frac{1}{N_1} \sum_{i=1}^N \frac{P_{i,1}^2}{(P_{i,1} + P_{i,2} e^b)^2} & \frac{1}{N_1} \sum_{i=1}^N \frac{P_{i,1} P_{i,2} e^b}{(P_{i,1} + P_{i,2} e^b)^2} \\ \frac{1}{N_2} \sum_{i=1}^N \frac{P_{i,1} P_{i,2} e^b}{(P_{i,1} + P_{i,2} e^b)^2} & \frac{1}{N_2} \sum_{i=1}^N \frac{P_{i,2}^2 (e^b)^2}{(P_{i,1} + P_{i,2} e^b)^2} \end{bmatrix} \quad (42)$$

Note that \mathbf{J}_b does not depend on λ , i.e., it is the same for all $\beta^* \in \mathcal{S}_b$, and so, the same the eigenvalues and eigenvectors. As a consequence, the behavior of the local dynamics at a fixed point results in an exact replica at every β^* . This fact proves item (i).

In order to obtain μ and \mathbf{v} , the matrix entries of (42) are written in terms of the auxiliary functions α_k , $k=1, 2$. By virtue of (12) and (27), the matrix in (42), becomes:

$$\mathbf{J}_b = \mathbf{J}_f([\lambda, \lambda+b]) = \begin{bmatrix} 1 + \alpha'_1(b) & -\alpha'_1(b) \\ 1 + e^b \alpha'_2(b) & -e^b \alpha'_2(b) \end{bmatrix} \quad (43)$$

The trace of \mathbf{J}_b equals the sum of its eigenvalues, so we have:

$$\mu = \alpha'_1(b) - e^b \alpha'_2(b) \quad (44)$$

Let $h(x)$ be the function on x defined as $h(x) = \alpha'_2(x) \alpha_1(x) - \alpha'_1(x) \alpha_2(x)$. By virtue of (34), we have that $h(x) \leq 0$ for all $x \in \mathbb{R}$. In particular, for $x = b$, and recalling that $\alpha_1(b) = 1$ and $\alpha_2(b) = e^{-b}$, it is valid that:

$$h(b) = \alpha'_2(b) \alpha_1(b) - \alpha'_1(b) \alpha_2(b) \leq 0 \quad (45)$$

$$\alpha'_2(b) - \alpha'_1(b) e^{-b} \leq 0 \quad (46)$$

$$\alpha'_2(b) e^b - \alpha'_1(b) \leq 0 \quad (47)$$

$$-\mu \leq 0 \quad (48)$$

Therefore, item (ii) is proven. As a consequence of μ being non-negative, any trajectory that approaches \mathcal{S}_b from one side does not cross to the other side.

For item (iii), on the one hand, the entries of \mathbf{J}_b in (42) satisfy:

$$N_1 J_{1,2} = N_2 J_{2,1} \quad (49)$$

then, the entries of \mathbf{J}_b in (43) meet:

$$-N_1 \alpha'_1(b) = N_2 (1 + e^b \alpha'_2(b)) \quad (50)$$

On the other, using (44) we have:

$$\text{Nul}(\mathbf{J}_b - \mu \mathbf{I}) = \text{Nul} \left(\begin{bmatrix} 1 + e^b \alpha'_2(b) & -\alpha'_1(b) \\ 1 + e^b \alpha'_2(b) & -\alpha'_1(b) \end{bmatrix} \right) \quad (51)$$

$$= \text{span} \{ [\alpha'_1(b), 1 + e^b \alpha'_2(b)] \} \quad (52)$$

$$= \text{span} \{ [N_2, -N_1] \} \quad (53)$$

Then, $E^s = \text{span} \{ \mathbf{v} = [N_2, -N_1] \}$. Note that, in case that $N_1 = N_2$, E^s and E^c become orthogonal.

4.2.4. Proof of Theo. 2

Theo. 1 shows that the fixed point set is a unitary slope straight line with intercept b . In particular, $\beta^* = [0, b]$ is a fixed point. The strategy for proving Theo. 2 depends largely on the geometrical interpretation of Lemma 1 which, in the case of two dimensions, means that any unitary straight line is mapped by \mathbf{f} onto another unitary straight line. The idea is to prove that any unitary slope straight line \mathcal{S}_x gets closer and closer to the fixed line \mathcal{S}_b with successive iterations of the map. So, the focus will be placed on the change of the corresponding intercepts. The demonstration starts with some auxiliary lemmas.

Lemma 7. *For all $x \in \mathbb{R}$, $\mathbf{f}^{(t)}(\mathcal{S}_x) \rightarrow \mathcal{S}_b$, as $t \rightarrow +\infty$*

Proof. Let $x \in \mathbb{R}$, and $\beta = [0, x]$. From (18), and using the auxiliary functions, we have that:

$$\mathbf{f}([0, x]) = [-\log \alpha_1(x), -\log \alpha_2(x)] \quad (54)$$

so by Lemma 1:

$$\mathbf{f}([0, x] + \boldsymbol{\lambda}) = \boldsymbol{\lambda} + [-\log \alpha_1(x), -\log \alpha_2(x)] \quad (55)$$

which, in terms of Def. 6, means that $\mathbf{f}(\mathcal{S}_x) = \mathcal{S}_{\phi(x)}$, where $\phi(x) = \log \left(\frac{\alpha_1(x)}{\alpha_2(x)} \right)$, i.e., the unitary slope straight line with x intercept, is mapped to the unitary slope straight line with $\phi(x)$ intercept.

This can be interpreted geometrically (see Fig. 2). Recursively, by applying Lemma 4 to $\phi(x) > b$, the same can be said of $\mathbf{f}^{(2)}(\mathcal{S}_x) = \mathcal{S}_{\phi^2(x)}$, where $\phi^2 = \phi \circ \phi$, and so on. In other words, for $x > b$, the succession of intercepts, $\{\phi^t(x)\}_{t \geq 1}$, is monotone decreasing and

$$\lim_{t \rightarrow +\infty} \phi^t(x) = b \quad (56)$$

In the analogous way, if $x < b$, $\mathcal{S}_{\phi(x)}$ will be placed between \mathcal{S}_b and \mathcal{S}_x , but *strictly* above the latter. Following the previous arguments, the succession $\{\phi^t(x)\}_{t \geq 1}$ is monotone increasing. \square

As a natural consequence of this lemma, it is possible to say that the orbit of any initial condition approaches \mathcal{S}_b .

Corollary 3. *For any $\beta^{[0]}$, $O^+(\beta^{[0]}) \rightarrow \mathcal{S}_b$, for $t \rightarrow +\infty$*

Proof. Indeed, any point, $\beta^{[0]} \in \mathbb{R}^2$, belongs to some \mathcal{S}_x , for some $x \in \mathbb{R}$. \square

With these results, it is shown that the fixed straight line \mathcal{S}_b is a global asymptotically stable set for \mathbf{f} . However, in order to demonstrate the convergence of SUCPA algorithm, it is still necessary to show that the orbit of any initial condition does not approach *asymptotically* to \mathcal{S}_b but, in fact, reaches a point β^* on it. Although it is already obvious that the asymptotic behavior is ruled out by the local dynamics illustrated in Fig. 1, we will also give a more rigorous argument on this point.

Let $\beta^{[t]}$ and $\beta^{[t+1]} = \mathbf{f}(\beta^{[t]})$ be two consecutive points of $O^+(\beta^{[0]})$. Let the increments, $\Delta_k(t) = \beta_k^{[t+1]} - \beta_k^{[t]}$, $k = 1, 2$. Then, the slope of the straight line through $\beta^{[t]}$ and $\beta^{[t+1]}$, is $\frac{\Delta_2(t)}{\Delta_1(t)}$.

Proceeding by *reductio ad absurdum*, if $O^+(\beta^{[0]})$ is asymptotic to \mathcal{S}_b , then the slopes must approach the unity:

$$\lim_{t \rightarrow +\infty} \frac{\Delta_2(t)}{\Delta_1(t)} = 1 \quad (57)$$

This claim is valid because of Cor. 2. Indeed, $O^+(\beta^{[0]})$ cannot cross over the straight line \mathcal{S}_b , and so the “oscillating” asymptotic approach cannot take place. From (19), it is obtained that:

- $\Delta_1(t) = 0$ if and only if $\Delta_2(t) = 0$ (and so, $\beta^{[t]} = \beta^{[t+1]}$)
- $\Delta_1(t) > 0$ if and only if $\Delta_2(t) < 0$
- $\Delta_1(t) < 0$ if and only if $\Delta_2(t) > 0$

Therefore, it results that $\frac{\Delta_2(t)}{\Delta_1(t)} < 0$ for all t , and this is in contradiction to (57).

Thus, having excluded the asymptotic behavior, there must be a fixed point, $\beta^* \in \mathcal{S}_b$, to which the orbit converges, and then, the proof of Theo. 2, for $K=2$, is completed.

5. Numerical examples

In this section we present three real-world applications, showing the features proved for the $K=2$ cases and the conjectures made for the $K=3$ case. The first two examples correspond to language models and the third to an image classification application. Implementation details can be found in the repository of this work².

5.1. Application to Language models with $K=2$

The first example corresponds to the calibration of the probabilities outputted by a language model when it is used as a zero-shot classifier. Specifically, a generative language model is a function that maps a string of characters x (the prompt) to a probability distribution $P_{LM}(t|x)$ over a set of tokens $V = \{t_1, \dots, t_{|V|}\}$ (the vocabulary), which represents the probability of the next token in the input string. Then, language models can be used as classifiers by computing the probability that the next token is the one that represents the class y to be predicted. For instance, we can compute the probability of the words “*positive*” or “*negative*” appears after the sentence “*Identify if the next review has a positive or negative connotation. Review: ‘I love this movie’. Sentiment:*”. This is an example of zero-shot classification because the prompt does not contain examples of correctly classified examples. In order to obtain a probability distribution $P(y_k|x)$ for each class y_k , we compute the score $s_k = P_{LM}(w_k|x)$ with a predefined set of tokens (in

²<https://github.com/LautaroEst/sucpa-convergence>

the example, the words $w_1 = \text{"positive"}$ and $w_2 = \text{"negative"}$) and then we normalized over all the scores:

$$P(y_k|x) = \frac{s_k}{\sum_{k=1}^K s_k} \quad (58)$$

This is a particularly good scenario of use-case because these probabilities are likely to be uncalibrated. For an extended explanation of this approach, see [10].

Two tasks were implemented following the above procedure. The one described here is usually called polarity classification and consists in determine if a given sentence has a positive or negative connotation. For this experiment, a subset of the SST-2 dataset, which contains examples of annotated movie reviews [18] was used. The number of positive and negative samples was $N_1 = 1729$ and $N_2 = 2271$, respectively. To obtain the class scores, the GPT-2 model [16] was used.

Using the above values of N_1 and N_2 and the probabilities outputted by the model, a line \mathcal{S}_b of fixed points with $b = -1.39726$ is obtained. Fig. 3 shows this line and the orbits of five different i.c.: $\beta_1^{[0]} = [0, 2]$ (in red), $\beta_2^{[0]} = [1.5, 3.5]$ (blue), $\beta_3^{[0]} = [3, 0]$ (cyan), $\beta_4^{[0]} = [4, -1]$ (green) and $\beta_5^{[0]} = [5, 1]$ (magenta). It can be appreciated that orbits starting at on one side of the line \mathcal{S}_b , converge to it on the same side, without crossing the semi-planes. Also, Lemma 1 and Corollary 1 are illustrated: The blue orbit initialized at $\beta_2^{[0]} = \beta_1^{[0]} + \lambda$, i.e. shifted from the red one (in the straight line direction), converges with the same shift, to $\beta_2^* = \beta_1^* + \lambda$. In addition, the convergence of the algorithm is really fast, managing to converge in at most 5 iterations.

5.2. Application to Language models with $K=3$

The second example, we repeat the same procedure to a classification task with $K = 3$. We choose the MNLI dataset [21], which contains examples of sentence pairs with textual entailment annotations. Specifically, given a premise sentence and a hypothesis sentence, the task is to predict whether the premise entails the hypothesis (entailment), contradicts the hypothesis (contradiction), or neither (neutral). The prompt template used for this task was the following: *“Premise: [premise]. Hypothesis: [hypothesis]. Entailment, neutral or contradiction? Answer:”* and the model used to obtain the probabilities was the same as the first experiment.

In this case, the parameter values are $N_1 = 1407$, $N_2 = 1298$ and $N_3 = 1295$. Fig. 4 shows the line of fixed points, $\mathcal{S}(\beta^*)$, with direction vector $[1, 1, 1]$; the

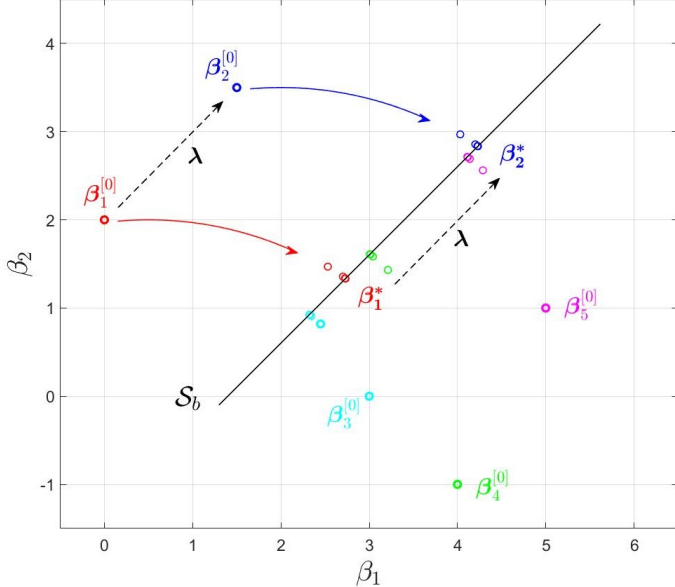


Figure 3: Example with $K=2$. Orbits of five different i.c.: $\beta_1^{[0]} = [0, 2]$ (red), $\beta_2^{[0]} = [1.5, 3.5]$ (blue), $\beta_3^{[0]} = [3, 0]$ (cyan), $\beta_4^{[0]} = [4, -1]$ (green) and $\beta_5^{[0]} = [5, 1]$ (magenta). Only five points of each orbit were plotted due to rapid convergence. The line of fixed points, S_b , with $b = -1.39726$. The shift vector $\lambda = [1.5, 1.5]$.

orbits of five different i.c.: $\beta^{[0]} = [1, -1, 1]$ (red), $\beta^{[0]} = [2, -2, 2]$ (blue), $\beta^{[0]} = [2.5, -2, 1]$ (magenta), $\beta^{[0]} = [2.5, -0.5, 1]$ (green) and $\beta^{[0]} = [1, -1.5, 1.5]$ (cyan).

As we mention in Conj. 1 and 2, all i.c. converges to the unique straight line of unitary slope. This example would seem to indicate that the characteristics shown for $K=2$ can be extended to a greater number of classes. In addition, the convergence of the algorithm is really fast, managing to converge in at most 5 iterations. Like the previous example, 5 steps of the algorithm are enough to achieve convergence.

5.3. Application to Image Classification

The final example shows that the features shown in the previous examples happen in other totally different applications. In this case, a recognizer of images of dogs and cats was trained on the Asirra dataset [9] obtained from

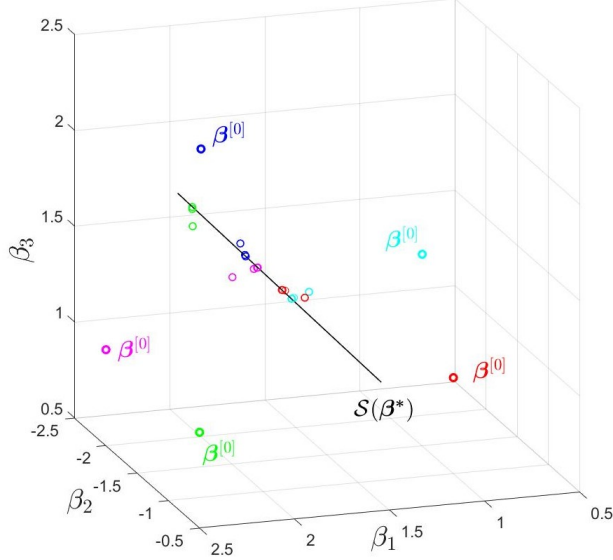


Figure 4: Example with $K = 3$. Orbits of five different i.c.: $\beta^{[0]} = [1, -1, 1]$ (red), $\beta^{[0]} = [2, -2, 2]$ (blue), $\beta^{[0]} = [2.5, -2, 1]$ (magenta), $\beta^{[0]} = [2.5, -0.5, 1]$ (green) and $\beta^{[0]} = [1, -1.5, 1.5]$ (cyan). Five points of each orbit are plotted. Also the line of fixed points, $S(\beta^*)$.

the Dogs-vs-Cats Kaggle competition website³. Here, the pretrained ResNet-18 [12] model was fine-tuned on 80% of the training data and validated on the rest. A final accuracy of 0.98 on the validation split was obtained after one epoch using Adam optimization with defaults parameters, a learning rate of 1e-4 and batch size of 64.

In this case, the parameter values are $N_1 = 10053$, $N_2 = 9947$ and $b = -0.03465$ is obtained. Fig. 5 shows the line of fixed points and the orbits of different i.c. The same conclusions as in the previous cases can be seen in this example with the difference that up to 200 steps were needed to achieve convergence. This is possibly because the algorithm was originally more uncalibrated (standard ResNet has a natural tendency to go out of calibration [11]).

³<https://www.kaggle.com/c/dogs-vs-cats>

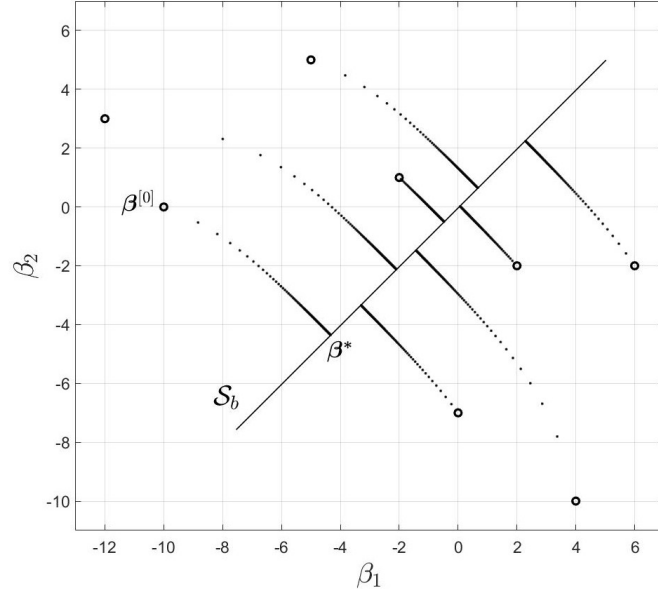


Figure 5: Example with $K=2$ in an image classification task. Orbits of eight different i.c. are plotted. At least 200 points of each one were needed to reach the corresponding limit point β^* .

6. Conclusions

In this work we proved several convergences properties of SUCPA, a calibration algorithm described by a non-hyperbolic map with a non-bounded set of non-isolated fixed points. Among them it is worth highlighting, on the one hand, the general results Cor. 1 and Lemma 2. The first one establishes that if there exists a fixed point, then, all points in the straight line of direction $[1, \dots, 1]$ and passing through it must be also fixed points of the map (an unbounded set of non-isolated fixed points); while the second one shows that the Jacobian matrix of the system is a regular transition probability matrix (for all $\beta \in \mathbb{R}^K$) which makes it a non-hyperbolic problem.

On the other hand, stronger conclusions were proved for the two-classes case by means of Theo. 1 which proves the existence and uniqueness of the fixed points straight line, and Theo. 2 which shows that every i.c. converges. These results seem to be valid for the general case, but it remains as future work to prove it formally. Additionally, interesting real-world application examples were presented in language models and image classification for which

all the mentioned results are experimentally corroborated.

References

- [1] Auger A, Akimoto Y, and Hansen N. An ODE method to prove the geometric convergence of adaptive stochastic algorithms. *Stochastic Processes and their Applications*, 145:269–307, 2022.
- [2] Niko Brümmer. *Measuring, refining and calibrating speaker and language information extracted from speech*. PhD thesis, Stellenbosch University, 2010.
- [3] Niko Brümmer and David A. Van Leeuwen. On calibration of language recognition scores. In *IEEE Odyssey - The Speaker and Language Recognition Workshop*, pages 1–8, 2006.
- [4] Tarłowski D. On asymptotic convergence rate of evolutionary algorithms. Technical report, <https://doi.org/10.36227/techrxiv.20103404.v2>, 2022.
- [5] Telmo de Menezes e Silva Filho, Hao Song, Miquel Perello Nieto, Raul Santos-Rodriguez, Meelis Kull, and Peter A Flach. Classifier calibration: a survey on how to assess and improve predicted class probabilities. *Machine Learning*, 112(9):3211–3260, 2023.
- [6] Robert Devaney. *An Introduction to Chaotic Dynamical Systems*. Addison-Wesley, 1987.
- [7] Jacob Devlin, Ming-Wei Chang, Kenton Lee, and Kristina Toutanova. BERT: Pre-training of deep bidirectional transformers for language understanding. In *Association for Computational Linguistics: Human Language Technologies*, pages 4171–4186, 2019.
- [8] Richard Duda, Peter Hart, and David Stork. *Pattern Classification*. John Wiley, 2 edition, 2001.
- [9] Jeremy Elson, John Douceur, Jon Howell, and Jared Saul. Asirra: A captcha that exploits interest-aligned manual image categorization. In *Proceedings of the 14th ACM Conference on Computer and Communications Security*, CCS ’07, page 366–374, New York, NY, USA, 2007. Association for Computing Machinery.

- [10] Lautaro Estienne, Luciana Ferrer, Matias Vera, and Pablo Piantanida. Unsupervised calibration through prior adaptation for text classification using large language models. *ArXiv*, abs/2307.06713, 2023.
- [11] Chuan Guo, Geoff Pleiss, Yu Sun, and Kilian Q. Weinberger. On calibration of modern neural networks. In *Proceedings of the International Conference on Machine Learning ICML*, Sydney, 2017.
- [12] Kaiming He, Xiangyu Zhang, Shaoqing Ren, and Jian Sun. Deep residual learning for image recognition. *CoRR*, abs/1512.03385, 2015.
- [13] Carl D. Meyer. *Matrix Analysis and Applied Linear Algebra*. SIAM, 2000.
- [14] J. Platt. Probabilistic outputs for support vector machines and comparison to regularized likelihood methods. In *Advances in Large Margin Classifiers*, 2000.
- [15] Jo Plested and Tom Gedeon. Deep transfer learning for image classification: a survey. *ArXiv*, abs/2205.09904, 2022.
- [16] Alec Radford, Jeff Wu, Rewon Child, D. Luan, Dario Amodei, and Ilya Sutskever. Language models are unsupervised multitask learners, 2019.
- [17] Li S. and Cheah Ch. Transfer learning algorithm for image classification task and its convergence analysis. In *IECON 2023- 49th Annual Conference of the IEEE Industrial Electronics Society*, 2023.
- [18] Richard Socher, Alex Perelygin, Jean Wu, Jason Chuang, Christopher D. Manning, Andrew Ng, and Christopher Potts. Recursive deep models for semantic compositionality over a sentiment treebank. In David Yarowsky, Timothy Baldwin, Anna Korhonen, Karen Livescu, and Steven Bethard, editors, *Proceedings of the 2013 Conference on Empirical Methods in Natural Language Processing*, pages 1631–1642, Seattle, Washington, USA, October 2013. Association for Computational Linguistics.
- [19] Jamieson William T. and Merino Orlando. Local dynamics of planar maps with a non-isolated fixed point exhibiting 1-1 resonance. *Advances in Difference Equations*, vol.142, 2018.

- [20] Stephen Wiggins. *Introduction to Applied Nonlinear Dynamical Systems and Chaos, 2nd. Ed.* Springer-Verlag, 2003.
- [21] Adina Williams, Nikita Nangia, and Samuel Bowman. A broad-coverage challenge corpus for sentence understanding through inference. In Marilyn Walker, Heng Ji, and Amanda Stent, editors, *Proceedings of the 2018 Conference of the North American Chapter of the Association for Computational Linguistics: Human Language Technologies, Volume 1 (Long Papers)*, pages 1112–1122, New Orleans, Louisiana, June 2018. Association for Computational Linguistics.